THE ASTROPHYSICAL JOURNAL, 455:88–95, 1995 December 10

THE CANADA-FRANCE REDSHIFT SURVEY. IV. SPECTROSCOPIC SELECTION EFFECTS AND 0300+00 FIELD SPECTROSCOPIC DATA

FRANCOIS HAMMER[1]
DAEC, Observatoire de Paris–Meudon, 92195 Meudon, France
DAVID CRAMPTON[1]
Dominion Astrophysical Observatory, National Research Council of Canada, Victoria, V8X 4MC Canada
OLIVIER LE FÈVRE[1]
DAEC, Observatoire de Paris–Meudon, 92195 Meudon, France
AND
SIMON J. LILLY[1]
Department of Astronomy, University of Toronto, Toronto, M5S 1A7 Canada
Received 1994 December 27; accepted 1995 June 19

ABSTRACT

Possible surface brightness selection effects in the redshift catalogs of the Canada-France Redshift Survey are investigated through comparisons of subsamples of the data. Our analyses demonstrate that the securing of redshifts is independent of possible biases arising from surface brightness effects and/or differing galaxy morphologies and orientations. The unusual geometry of the mask designs for our spectroscopic observations also do not produce any significant bias. There is, however, a bias at the highest and lowest redshifts, especially for absorption-line galaxies at $z > 1$ and $z < 0.2$, due to the adopted spectral range (4250–8500 Å). Apart from the latter, we conclude that our sample of identified galaxies is an unbiased subsample of the original photometric catalog and is essentially limited by I-band flux density ($17.5 \leq I_{AB} \leq 22.5$). Finally, spectroscopic data for the remaining CFRS field is presented. Data for 273 objects in the 0300+0000 field are given.

Subject headings: catalogs — galaxies: distances and redshifts — methods: observational

1. INTRODUCTION

The CFRS project has been a major effort to gather a complete sample of ~ 1000 spectra of very faint field objects ($I_{AB} \leq 22.5$) (The AB magnitude system is used throughout this paper; $I_{AB} = I + 0.48$). The main goals of this survey and a discussion of the establishment of reliable photometric catalogs made prior to the spectroscopy are given by Lilly et al. (1995, hereafter CFRS I). Our deep imaging provides a sample of galaxies with isophotal $I_{AB} \leq 22.5$, which is substantially complete for central surface brightness as faint as $\mu(I) = 24.5$. Le Fèvre et al. (1995, hereafter CFRS II) describe the fundamental methodology adopted for our spectroscopy, and Lilly et al. (1995, hereafter CFRS III) discuss the accuracy and reliability of our redshift measurements. Here we present the last set of spectroscopic data of the CFRS (in the 0300+00 field) and discuss possible selection effects related to our spectroscopy, which might affect the statistical properties of the resulting sample.

Several aspects of the methodology of our spectroscopic program could conceivably have led to differences in the ease with which spectroscopic identifications were secured. Two obvious possibilities are related to object morphology and surface brightness, since peculiar galaxy morphologies could cause a smaller fraction of their light to pass through the spectrograph slit, and the unidentified objects might be expected to be predominantly low surface brightness galaxies or very elongated galactic disks orientated perpendicular to the slits. In addition, the unusual mask geometry (three strips of slits per mask; see CFRS II) could potentially lead to a redshift bias since the bright zero-order contamination from objects in the adjacent strips tends to affect a particular range of wavelengths in the spectra. In this paper we investigate surface brightness selection effect in § 2, selection effect related to the galaxy orientation relatively to the slit in § 3, and selection effect coming from our mask geometry in § 4, and we conclude that they are all in fact insignificant.

In § 5, we discuss one selection effect that is, however, almost certainly present in the sample. This arises from the finite wavelength range of the spectra which makes the spectroscopic identification of absorption-line objects at very high and very low redshifts difficult.

Finally, we present in § 6 the spectroscopic catalog for 273 objects in the 0300+00 survey field.

2. SURFACE BRIGHTNESS SELECTION EFFECTS

Uncontrolled selection biases against low surface brightness galaxies might cause severe biases in the determination of the luminosity function. For example, it has been suggested that the Loveday et al. (1992) local luminosity function might be biased against low surface brightness galaxies (Ferguson & McGaugh 1995), which might affect the corresponding slope at faint luminosities. For the CFRS project, objects were selected to have isophotal $17.5 \leq I_{AB} \leq 22.5$ from very deep images. This procedure should produce an unbiased sample that includes nearly all objects with central surface brightness as faint as $\mu(I) = 24.5$ (see CFRS I). Selection of the objects for spectroscopy was done without regard to the morphological properties of an object. "Blind" techniques were used for selecting objects from the photometric catalog (i.e., without regard-

[1] Visiting Astronomer, Canada-France-Hawaii Telescope, which is operated by the National Research Council of Canada, the Centre de Recherche Scientifique of France, and the University of Hawaii.

ing their brightness and compactness), and strict criteria, independent of the object surface brightness, were applied to reject spectra for instrumental reasons (see CFRS II). We examine here whether objects for which we have failed to assign a redshift are preferentially the lowest surface brightness galaxies, for which one might expect relatively low signal-to-noise ratio (S/N) per pixel on their two-dimensional spectra.

We have tested this hypothesis by comparing the surface brightness properties of two different samples, the first one containing the galaxies with a secure redshift identification (confidence class ≥ 2) and the second one consisting of all objects for which we failed to obtain a secure spectroscopic identification. Figure 1 shows the histograms of the distribution of the compactness of the objects in these two samples parameterized by $[\mu_{AB}(I) - I_{AB}]$ (see CFRS I) in three different magnitude ranges. While the distributions of the two samples, identified galaxies and unidentified objects, differ slightly from one another (e.g., in the $21 < I_{AB} < 22$ range), the overall success rate in identifying a galaxy redshift is independent of the compactness. Even at the faintest magnitudes, there is no evidence for any systematic biases for or against galaxies with central surface brightness as faint as $\mu(I) = 24.5$ in our final spectroscopic sample relative to the photometric one. As noted in CFRS I, virtually all the $I_{AB} \leq 22.5$ "normal" galaxies should have central surface brightnesses higher than this value.

3. ELONGATED GALAXIES ORIENTED PERPENDICULAR TO THE SLIT

Another bias in the spectroscopic identifications might arise from highly elongated sources (e.g., edge-on disks) that lie perpendicular to the slit. We generate a simple test, again by comparing the properties of two samples, one containing the galaxies with a secure redshift identification (classification ≥ 2), and the other including all the objects for which we failed to secure a spectroscopic identification. The distribution of a simple geometric parameter which accounts for the object elongation as well as for the major axis orientation relative to the slit was then investigated.

Assuming e is the source eccentricity and θ is the major axis orientation angle relative to the slit, the ratio of the one-

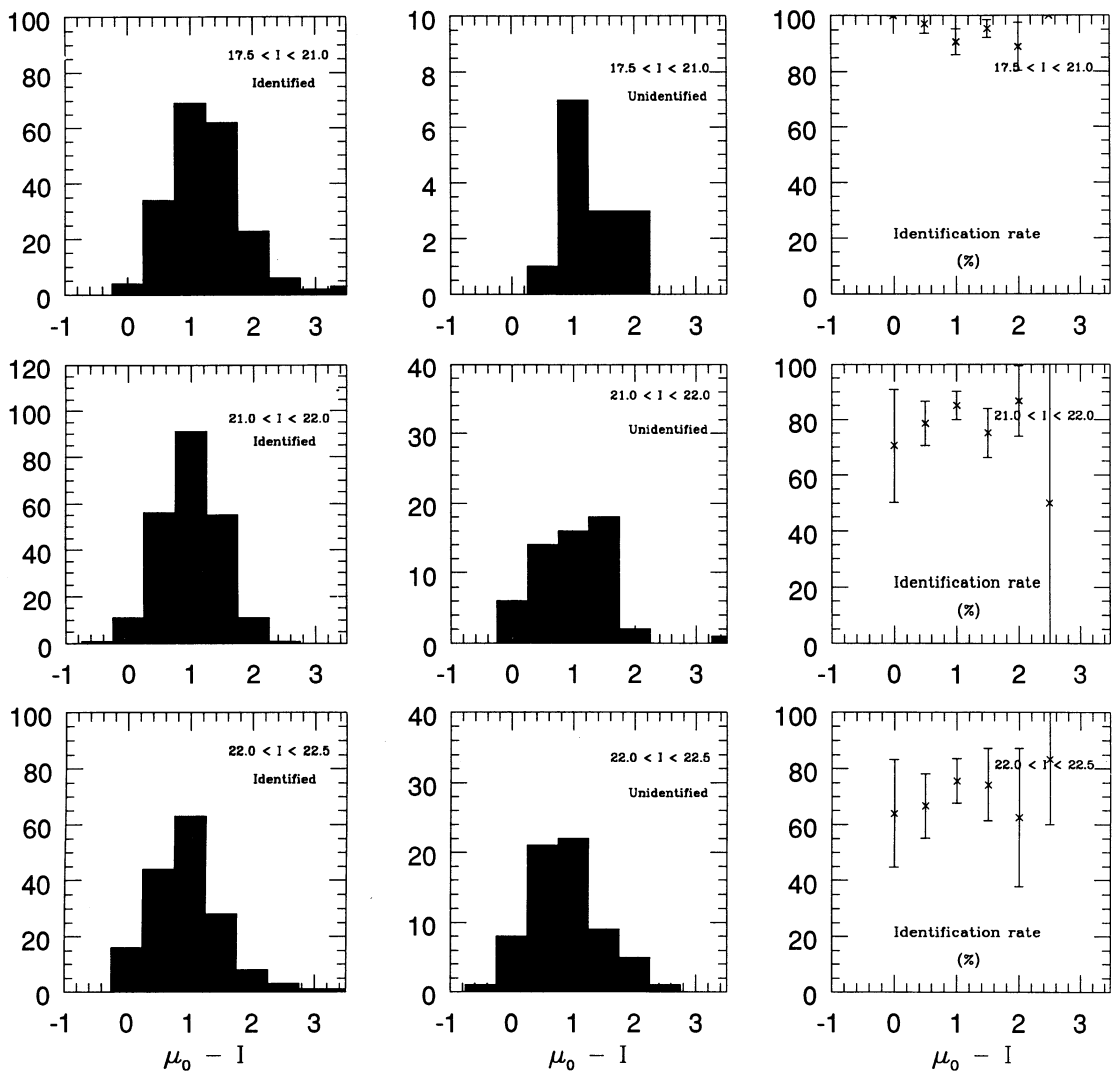

FIG. 1.—Histograms of the distribution of the compactness parameters for identified galaxies and unidentified objects in three different magnitude bins. The three panels on the right show the corresponding identification rates; the error bars are based on an assumed Poissonian distribution.

dimensional source section crossed by the slit to the source radius, $f = [(1 - e^2 \cos^2 \theta)/(1 - e^2)^{1/2}]^{1/2}$, is an appropriate estimator of the orientation effect. For circular sources $f = 1$; for sources having their major axis along the slit length ($\theta = 90°$) $f > 1$; and as the eccentricity and the orientation angle decreases $f < 1$. The orientation effect could potentially affect all those sources with isophotal diameters ($2 \times r_{28}$) larger than the slit width (1".75), and so e and θ were measured in a homogeneous way for all such objects in the 00^h, 03^h, and 10^h fields. Figure 2 presents the distribution of the identified galaxies and unidentified objects for various values of the f parameter. There is no evidence that these distributions differ significantly, which implies the absence of any systematic bias for or against elongated sources in our spectroscopic sample.

4. ZERO-ORDER CONTAMINATION

The peculiar geometry of our mask design (three strips of slits; see CFRS II) led us to investigate whether this could have been introduced biases in our spectroscopic sample. CFRS II (Fig. 1) shows that most of the zero orders are superposed on the blue part of the spectra (mostly below 5500 Å) and thus severely contaminate a wavelength range of 200–300 Å. The zero orders' contamination can cause difficulties in recognizing some of the most common features (e.g., [O II] λ3727 and the 4000 Å break) found in galaxy spectra. This could, in turn, affect the identification of absorption-line galaxies with $z < 0.38$ or emission-line galaxies with $z < 0.48$.

Since the putative zero orders can affect only the spectra in the two lower strips of spectra, comparison of the unidentified fraction of objects with that for objects in the top row should reveal any bias. Figure 3 demonstrates that no such bias is present. Furthermore, the redshift histograms for the identified galaxies located in the top rows in the different masks are identical to those for the galaxies in the two lower strips. For instance, the fraction of galaxies with $z < 0.48$ in the top strip (65 of 174) is very similar to that for the two bottom strips (155 of 418 galaxies). We thus conclude that there is no significant bias arising from overlapping zero orders.

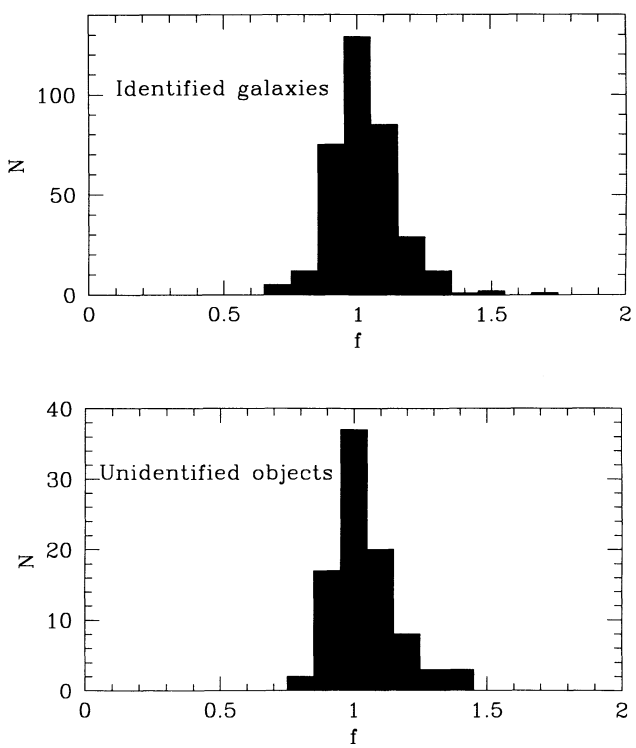

FIG. 2.—Histograms of the parameter f which describes the effect of orientation on the amount of light entering a slit ($f > 1$ means that the source main axis is preferentially oriented along the slit, and $f < 1$ indicates that it lies perpendicular to the slit). There is no evidence that the two populations (identified galaxies and unidentified objects) have different distributions.

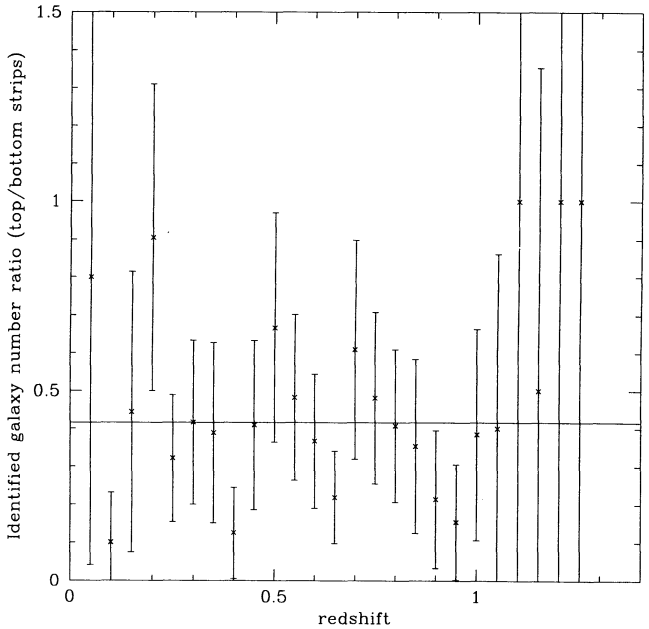

FIG. 3.—The ratio $R = N$(galaxies in the top strips)/N(galaxies in the bottom strips) vs. redshift. Redshift bins of 0.05 were adopted. The horizontal line shows the expected ratio, 174/418 = 0.416.

5. BIASES RELATED TO OBSERVED SPECTRAL RANGE

The most important selection effect expected in any spectroscopic work of this kind is caused by the unavoidable limitation of the spectral range. A relatively large spectral range was used for CFRS, from 4250 Å to 8500 Å (see CFRS II). Our spectra show that there are basically no features that are useful for redshift identification below 3727 Å at rest (or below 4000 Å at rest for an absorption-line galaxy). This is clearly a limitation of our survey, since identification of $z > 1.28$ emission-line galaxies or $z > 1$ absorption-line galaxies is virtually impossible from our spectra. A quantitative estimation of this selection effect will be presented in Crampton et al. (1995, hereafter CFRS V).

The detection of spectral features in the blue region of our spectra is limited by the decreasing efficiency of the CCD below 4500 Å rather than by our spectral wavelength limit (4250 Å). It results in a reduced efficiency, especially in identifying red absorption-line galaxies at low redshift ($z < 0.2$). Indeed, in our complete sample, we have identified no such galaxies at $z < 0.15$, while four would be expected from the number identified at higher redshift. Although the number of objects possibly affected is small because of the small volumes accessible in our survey, the shape and errors of the derived luminosity function at low redshift could obviously be affected.

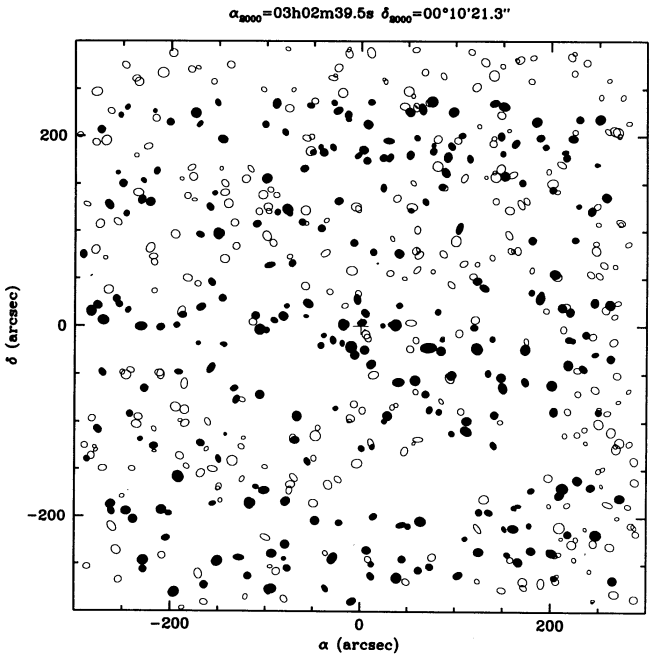

FIG. 4.—Finding chart for objects in the 0300+000 field. Eccentricities and orientations are those described in the text (§ 3). Filled symbols represent objects for which spectra were obtained (see Table 1). North is at the top, and east to the left.

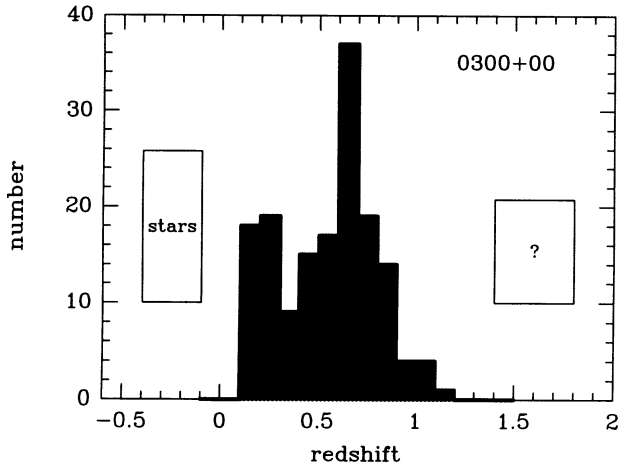

FIG. 6.—Redshift histogram of the identified galaxies (confidence class ≥ 2) in the 0300+000 field. Boxes represent relative numbers of stars and unidentified objects (confidence class ≤ 1).

6. SPECTROSCOPIC DATA IN THE 0300+00 FIELD

This field is located at $\alpha(2000) = 03^h02^m39^s.5$ and $\delta(2000) = 00°10'21''.3$. A finding chart is shown in Figure 4, and a gray-scale reproduction showing the observed objects is shown in Figure 5 (Plate 7). In this field there are 611 objects with $17.5 \leq I_{AB} \leq 22.5$, and we obtained spectra for 271 (44%) of them. We also obtained spectra of two objects at a fainter magnitude level. The statistically complete sample (see CFRS II) contains 252 objects, including 48 stars and two QSOs. The success rate in redshift identification (confidence class ≥ 2) is 82.5%, the average redshift is 0.54, and the corresponding redshift distribution is shown in Figure 6.

Several observational problems (poor blue coating on the CCD and cirrus; see CFRS II) were experienced during the first observations (five masks in 1992 October, 1992 December, and 1993 February) of this field. These spectra were thus poorer than average, and the overall redshift identification rate (with confidence class ≥ 2) fell to $\sim 60\%$. Many of these objects were reobserved with three new masks (6, 7, and 8), designed to include most of the unidentified objects in masks 1, 2, 4, and 5. Objects in mask 3 were abandoned since its quality was so poor. These reobservations plus a careful analysis of the data (including co-addition of spectra of the same object observed several times) allowed us to reach an identification rate comparable to that of the other fields.

Table 1 presents the data for the 0300+000 field. The first part lists the objects which constitute our complete sample (see CFRS II), and the second part contains objects classified in the supplementary catalog. The first column gives the object CFRS name, columns (2) and (3) give the 2000 coordinates, column (4) gives the isophotal I_{AB} magnitude, column (5) gives the $(V-I)_{AB}$ color index, column (6) gives the compactness parameter (see CFRS I), and columns (7) and (8) list the object redshift (0.000 for a star) and the corresponding confidence classes (class 0, no identification; class 1, poor confidence in the redshift; classes 2, 3, and 4, confidence levels higher than 85%, 99%, and 100%, respectively; and classes 8 and 9, single emission-line objects; see CFRS II). A list of the spectral features used to determine the redshift is given in the final columns of the table.

7. CONCLUSION

This paper completes a series of three papers which present the spectroscopic data of the CFRS and discuss the methodology and the limitations of our spectroscopic work. In this paper, possible biases are explored that might have originated from our observational methods. It is demonstrated that our strategy, adopted to optimize our multiplexing gain (i.e., three strips of slits per observing mask), has apparently not affected our identification of galaxies at moderate z, even though bright zero orders contaminate ~ 200 Å in the blue part of many spectra. The surface brightnesses, orientations, and eccentricities of the unidentified objects compared to those of the identified galaxies show that any biases related to these properties are also insignificant. Apart from small biases at the lowest and highest redshift regimes arising from the limited wavelength range (4250–8500 Å) of our spectra, our final spectroscopic catalog is essentially unbiased relative to the original photometric sample from which it was selected and is limited by one single selection criterion, the I-band flux density.

We thank the directors of the CFHT and the two allocation time committees (CFGT and CTAC) for their continuing support and encouragement. S. J. L.'s research is supported by the NSERC of Canada. We acknowledge some travel support from NATO.

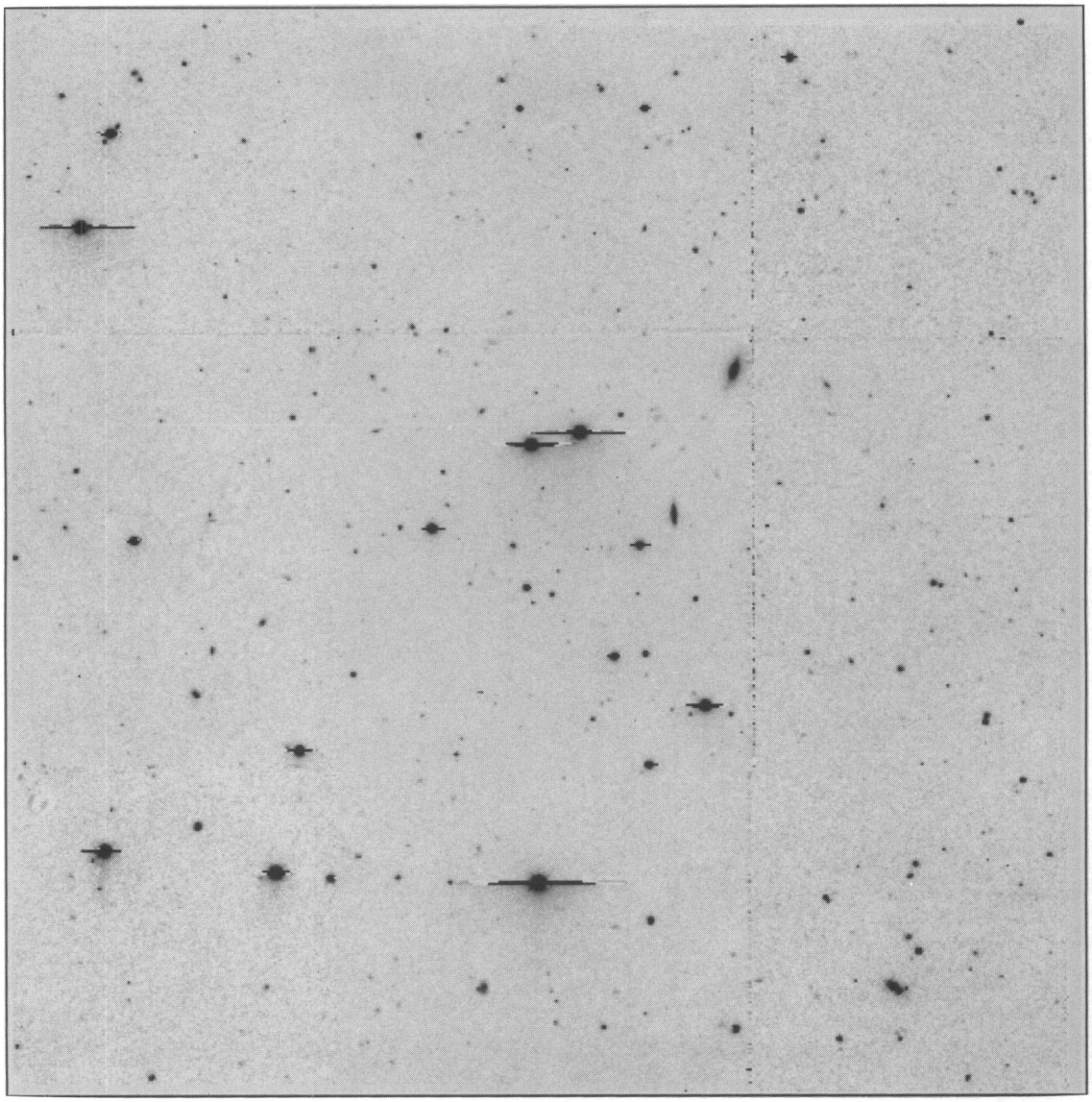

FIG. 5.—A gray-scale image of the 0300 + 000 field

HAMMER et al. (see 455, 91)

TABLE 1

SPECTROSCOPIC CATALOG IN THE 0300+00 FIELD

CFRS	RA[2000]	δ[2000]	I_{AB}[a]	$(V-I)_{AB}$[b]	Q[c]	z	C[d]	Spectroscopic features[e]
03.0003	03 02 31.85	+00 13 18	22.49	1.31	9.86	0.2205	4	4863 4959 5007 6562
03.0029	03 02 30.13	+00 14 16	22.24	1.46	2.64	...	0	
03.0032	03 02 29.68	+00 13 41	20.96	2.45	2.12	0.5220	3	3727 3933 3969 4000 4304 4959
03.0035	03 02 29.41	+00 12 59	21.16	2.68	2.54	0.8800	1	3727
03.0037	03 02 29.48	+00 14 13	19.69	1.26	1.79	0.1730	3	6562 6725
03.0046	03 02 28.67	+00 13 33	20.79	1.97	3.23	0.5120	3	3727 3969 4102 4304
03.0053	03 02 28.19	+00 12 52	22.23	1.43	3.78	0.2000	1	1
03.0062	03 02 27.20	+00 13 56	20.96	1.93	2.84	0.8252	3	3727 3969 4102 1
03.0063	03 02 26.95	+00 13 39	21.09	3.50	1.09	0.0000	4	
03.0068	03 02 26.58	+00 13 30	21.69	3.00	1.06	0.0000	3	
03.0075	03 02 26.08	+00 12 45	22.02	1.85	1.74	0.5100	2	3969 4304 1
03.0085	03 02 25.24	+00 13 24	22.00	1.35	2.43	0.6100	4	3727 3933 3969 4102 4863 5007
03.0087	03 02 25.14	+00 13 19	21.92	1.83	1.93	0.2170	2	4304 4863 6562
03.0090	03 02 24.69	+00 13 38	20.94	1.92	2.39	0.5260	1	3969 4000
03.0096	03 02 24.29	+00 12 28	22.14	0.93	1.10	0.2173	4	3727 3934 3969 4863 4959 5007 6562
03.0098	03 02 24.23	+00 13 59	21.48	1.92	1.91	0.5010	3	3727 3933 3969 4304 5175
03.0106	03 02 23.04	+00 13 12	21.03	1.03	1.10	2.0700	13	1549 1909
03.0111	03 02 22.81	+00 13 59	19.24	1.71	1.01	0.0000	4	5175 5892
03.0114	03 02 22.36	+00 12 37	21.00	1.99	3.17	0.2800	1	4000 5175
03.0125	03 02 31.52	+00 10 20	22.08	2.08	6.95	0.7900	3	3727 3837 3885 3969 1
03.0131	03 02 31.32	+00 09 58	20.98	2.05	3.71	0.6510	4	3933 3969 4000 4304 4863
03.0133	03 02 31.31	+00 11 09	22.45	1.00	3.23	1.0480	9	3727
03.0138	03 02 30.82	+00 11 01	20.09	2.03	1.83	0.4780	4	3933 3969 4000 4102 4340 5175
03.0142	03 02 30.53	+00 09 32	21.92	2.97	1.49	0.0000	2	
03.0145	03 02 30.24	+00 10 08	21.57	0.99	2.98	0.6052	4	3727 4959 5007
03.0146	03 02 30.09	+00 08 49	22.46	1.22	2.02	0.8590	8	3727 1
03.0148	03 02 29.63	+00 09 28	18.49	2.55	1.04	0.0000	4	
03.0149	03 02 29.51	+00 09 17	20.74	0.59	4.22	0.2526	4	3727 4863 5007 6562 6583 6725
03.0165	03 02 27.96	+00 09 23	20.04	0.40	1.95	0.1770	4	3727 3868 4340 4863 4959 5007 6300
03.0167	03 02 27.96	+00 09 57	20.67	1.54	2.22	0.6020	4	3727 3933 3969 4102 4304 4340 5175
03.0174	03 02 27.53	+00 10 57	22.31	1.62	2.06	0.5255	2	3727 3887 3969 4304 5175
03.0176	03 02 27.48	+00 11 51	20.92	2.00	1.79	0.4975	3	3934 3969 4000 4304 5175
03.0184	03 02 26.93	+00 10 50	19.65	2.57	1.67	0.0000	4	
03.0186	03 02 26.86	+00 10 55	22.01	1.87	1.76	0.5220	2	3727 1
03.0196	03 02 25.97	+00 08 52	21.96	0.60	1.90	0.2580	1	4102 1
03.0201	03 02 25.92	+00 11 16	21.21	0.81	1.48	0.0000	2	5175
03.0210	03 02 25.41	+00 10 41	21.64	1.93	2.71	...	0	
03.0218	03 02 24.98	+00 09 41	20.42	2.50	2.34	0.6478	3	3933 3969 4000 4102 4304
03.0223	03 02 24.85	+00 10 36	21.59	1.84	2.84	...	0	
03.0226	03 02 24.66	+00 10 06	18.86	0.68	1.02	0.0000	4	5892 6562
03.0233	03 02 24.53	+00 11 52	20.93	2.95	1.04	0.0000	4	
03.0241	03 02 23.94	+00 09 37	22.02	0.59	2.84	0.2896	3	3727 4959 5007 6562
03.0246	03 02 23.75	+00 10 13	20.49	2.64	1.05	0.0000	4	
03.0260	03 02 23.38	+00 12 22	21.61	2.85	1.86	0.8040	2	3933 3969 4102
03.0261	03 02 23.16	+00 10 46	21.75	1.93	1.84	0.6997	4	3727 3933 4000 4102 4304 5007
03.0262	03 02 22.87	+00 08 51	17.65	2.57	0.85	0.0000	4	
03.0286	03 02 22.01	+00 09 47	21.00	2.28	2.04	0.7860	3	3933 3969 4000 4304
03.0287	03 02 22.08	+00 10 44	19.02	2.30	1.05	0.0000	4	
03.0315	03 02 31.16	+00 06 24	20.28	1.40	12.87	0.2228	4	3727 3934 3969 4863 4959 5007 6562
03.0316	03 02 31.15	+00 07 07	21.98	2.91	3.20	0.8150	3	3727 3837 3969 4102
03.0321	03 02 30.46	+00 07 06	21.67	3.80	1.70	...	0	
03.0323	03 02 30.15	+00 08 17	22.50	1.26	3.68	...	0	
03.0327	03 02 29.18	+00 06 21	21.89	1.40	1.90	0.6064	3	3727 3969 3885
03.0332	03 02 28.77	+00 06 49	21.88	0.53	2.00	0.1877	4	3727 3969 4863 4959 5007 6562 6725
03.0334	03 02 28.72	+00 07 11	18.28	2.41	1.12	0.0000	4	
03.0337	03 02 28.42	+00 06 14	21.70	1.30	2.82	0.3605	3	3727 4959 5007
03.0346	03 02 27.67	+00 06 52	21.88	1.35	1.84	...	0	
03.0349	03 02 27.53	+00 06 26	20.44	2.16	1.23	0.0000	4	
03.0350	03 02 27.53	+00 07 29	20.99	2.36	1.78	0.6950	3	3837 3885 3934 3969 4000 4304 4863
03.0359	03 02 25.92	+00 05 57	20.79	1.28	3.92	...	0	
03.0365	03 02 25.56	+00 07 25	19.19	1.03	2.36	0.2187	4	5175 6562 6725
03.0377	03 02 24.32	+00 07 40	20.72	1.01	1.34	0.0000	3	5175
03.0384	03 02 23.40	+00 07 33	21.49	1.98	1.90	...	0	
03.0387	03 02 23.05	+00 06 43	19.75	1.45	3.09	0.3760	2	3933 3969 4304 5175 1
03.0393	03 02 21.85	+00 05 54	21.62	0.45	2.92	0.1649	3	4863 4959 5007 6562 6725
03.0400	03 02 21.38	+00 07 21	20.16	2.39	1.88	0.6560	3	3933 3969 4000 4340 4962
03.0422	03 02 46.29	+00 13 53	21.21	1.38	1.95	0.7148	3	3727 3837 3969 4102
03.0423	03 02 46.18	+00 12 57	19.00	0.75	1.00	0.0000	4	5175 6562
03.0436	03 02 45.40	+00 12 21	21.82	0.69	1.98	0.2066	2	5007 6562
03.0437	03 02 45.51	+00 14 15	22.05	3.23	1.48	0.0000	2	
03.0442	03 02 44.89	+00 13 45	21.44	0.97	2.20	0.4776	3	3727 3885 3969 5007
03.0443	03 02 44.69	+00 12 24	19.48	-0.02	1.97	0.1178	4	4102 4340 4863 4959 5007 6300 6562
03.0445	03 02 44.57	+00 12 20	20.64	0.64	2.59	0.5300	3	3727 3934 3969 4102
03.0466	03 02 43.52	+00 13 07	22.47	0.94	2.66	0.5304	3	3727 4863 5007
03.0480	03 02 42.92	+00 13 24	22.12	0.87	3.12	0.6079	3	3727 4959 5007
03.0485	03 02 42.38	+00 13 29	22.22	0.77	1.22	0.6056	4	3727 3868 4102 4340 4863 4959 5007
03.0488	03 02 42.16	+00 13 24	21.58	0.87	1.79	0.6069	4	3727 3868 4863 5007
03.0494	03 02 41.50	+00 13 29	22.42	0.54	2.84	0.2230	2	3727 6562 1
03.0496	03 02 41.44	+00 14 16	20.99	0.53	0.98	0.0000	4	5175 5892

TABLE 1—*Continued*

CFRS	RA[2000]	δ[2000]	I_{AB} [a]	$(V-I)_{AB}$ [b]	Q [c]	z	C [d]	Spectroscopic features [e]
03.0500	03 02 41.08	+00 12 33	20.67	0.55	3.64	0.1510	3	3969 4304 5175 6562 6583 6725
03.0501	03 02 41.16	+00 14 08	21.85	1.77	2.22	···	0	
03.0507	03 02 40.44	+00 14 03	20.95	0.77	2.08	0.4660	3	3727 3889 3969 4102 4863 5007
03.0508	03 02 40.42	+00 13 59	21.92	0.46	1.49	0.4642	4	3727 4340 4863 4959 5007
03.0523	03 02 39.34	+00 13 27	21.31	1.10	1.81	0.6508	4	3727 4863 4959 5007
03.0528	03 02 39.10	+00 13 16	21.34	1.78	1.79	0.7140	3	3969 4000 1
03.0531	03 02 39.04	+00 13 53	21.08	2.87	1.00	0.0000	4	
03.0533	03 02 38.80	+00 14 17	21.47	1.34	2.98	0.8290	3	3727 3868
03.0545	03 02 37.93	+00 12 47	21.69	0.46	2.74	0.1720	1	4304 5175 5892 6562 1
03.0546	03 02 37.94	+00 13 18	21.04	1.31	0.99	0.0000	4	5175 6562
03.0550	03 02 37.58	+00 13 36	21.89	0.33	49.39	0.2790	1	3727 1
03.0551	03 02 37.49	+00 13 19	22.21	1.72	3.68	···	0	
03.0560	03 02 36.00	+00 12 23	21.25	2.45	1.56	0.6968	3	3933 3969 4000 4304 4863 1
03.0562	03 02 36.06	+00 13 21	19.91	0.37	2.82	0.1689	4	4863 4959 5007 6562 6725
03.0564	03 02 36.08	+00 14 06	20.36	1.22	1.68	0.2990	3	3837 3933 3969 4304 5175 6562
03.0570	03 02 35.58	+00 13 39	22.07	1.21	1.22	0.6480	3	3727 3934 3969 4000 1
03.0578	03 02 35.19	+00 14 10	20.79	0.48	4.55	0.2200	3	5007 6562 6725
03.0579	03 02 34.97	+00 12 32	22.01	1.38	2.39	0.6600	2	3933 3969 4000
03.0587	03 02 34.43	+00 13 25	22.31	0.76	2.48	0.9720	9	3727
03.0588	03 02 34.50	+00 14 18	19.95	2.59	1.39	0.0000	4	
03.0589	03 02 34.41	+00 13 31	22.18	1.37	1.35	0.7160	3	3727 3969
03.0595	03 02 33.81	+00 12 48	21.46	1.33	1.48	0.6061	4	3727 3969 4102 4863
03.0599	03 02 33.55	+00 13 03	21.19	0.84	2.54	0.4805	4	3727 3969 4863 5007 1
03.0602	03 02 33.42	+00 13 19	20.44	1.90	1.13	0.0000	4	
03.0603	03 02 33.14	+00 13 31	20.56	0.49	1.55	1.0480	14	2799 3426 3727 3969 4102
03.0605	03 02 33.01	+00 14 07	21.28	0.36	2.64	0.2193	4	3727 4863 4959 5007 6562 6725
03.0615	03 02 32.41	+00 13 42	22.01	0.96	4.22	1.0480	9	3727
03.0619	03 02 46.92	+00 10 32	20.80	0.40	2.24	0.4854	3	3727 3837 3887 3969 4000 4340 5175
03.0624	03 02 46.59	+00 09 09	18.39	1.40	1.36	0.0000	4	
03.0625	03 02 46.62	+00 10 18	19.86	2.68	1.16	0.0000	4	
03.0632	03 02 46.17	+00 10 17	22.50	0.73	2.57	···	0	
03.0641	03 02 45.93	+00 11 25	20.03	1.24	3.58	0.2630	4	3727 3837 3934 3969 4304 6562 6725
03.0645	03 02 45.61	+00 10 27	21.36	0.77	1.95	0.5275	4	3727 3969 4192 4340 4863 4959 5007
03.0657	03 02 44.97	+00 10 31	19.23	2.53	1.09	0.0000	4	
03.0660	03 02 44.72	+00 10 42	22.35	0.80	2.02	0.3954	3	3727 3969 4304 4863 5007
03.0668	03 02 44.11	+00 08 22	21.35	2.13	2.24	···	0	
03.0672	03 02 44.34	+00 11 27	22.09	1.46	3.23	0.6860	2	3969 4102 1
03.0676	03 02 43.98	+00 08 47	20.77	2.35	1.84	0.5280	3	4000 3933 3969 4102 4304 5175
03.0692	03 02 43.22	+00 10 45	20.46	0.63	2.59	1.0830	9	3727 1
03.0711	03 02 42.31	+00 10 01	21.04	0.78	1.83	0.2620	3	3934 3969 4000 6562 6725
03.0716	03 02 42.11	+00 10 11	22.49	4.25	1.10	0.0000	3	
03.0717	03 02 42.28	+00 12 04	20.95	1.60	2.82	0.6070	3	3934 3969 4000 4102 4863
03.0726	03 02 41.46	+00 10 07	21.79	0.18	2.76	0.1354	4	4863 5007 6562 6725
03.0728	03 02 41.26	+00 08 55	22.07	2.11	1.15	0.5200	3	3969 4000 4304 4863 1
03.0743	03 02 40.73	+00 10 23	19.21	1.83	1.98	0.4656	4	3837 3933 3969 4102 4304 4863
03.0757	03 02 39.92	+00 09 51	20.48	3.44	1.11	0.0000	4	
03.0759	03 02 40.00	+00 11 49	21.07	2.73	1.06	0.0000	4	
03.0761	03 02 39.75	+00 10 49	21.91	1.48	3.82	0.8215	2	3969 4000 4102
03.0767	03 02 39.42	+00 10 25	21.65	2.26	2.45	0.6690	3	3727 3969 4000 4304
03.0772	03 02 39.22	+00 09 56	18.40	0.52	1.43	0.0000	3	4863 5175 6562
03.0776	03 02 39.18	+00 10 35	22.37	1.10	1.71	0.8830	8	3727 1
03.0786	03 02 38.76	+00 09 41	21.65	0.95	2.10	0.3975	4	3727 4000 3969 4102 4304 5007
03.0790	03 02 38.63	+00 11 39	21.94	1.04	1.53	···	0	
03.0803	03 02 37.81	+00 08 42	22.10	2.22	1.28	0.5800	1	4304 4863
03.0806	03 02 37.95	+00 10 22	22.03	1.97	1.04	0.0000	2	
03.0811	03 02 37.59	+00 08 48	19.85	2.02	2.20	0.4826	4	3933 3969 4000 4304 4863 5175
03.0825	03 02 37.41	+00 10 23	22.09	0.33	1.23	0.0000	2	4863 5175
03.0837	03 02 37.05	+00 10 22	21.77	2.74	2.74	0.8215	3	3727 3969 4000 4102 4304
03.0844	03 02 36.79	+00 10 43	21.87	2.25	1.76	0.8220	3	3934 3969 4000 4102 4304
03.0846	03 02 36.81	+00 11 38	18.72	2.48	1.10	0.0000	4	
03.0860	03 02 35.67	+00 09 25	17.66	1.22	0.87	0.0000	4	5175 5892
03.0879	03 02 34.90	+00 09 10	22.48	0.96	2.57	0.6013	2	3727 4102 1
03.0883	03 02 34.63	+00 08 54	20.98	2.30	1.91	0.6020	3	3934 3969 4000 4102
03.0898	03 02 33.95	+00 08 52	20.48	0.46	1.09	0.0000	4	4863 5175 6562
03.0905	03 02 33.84	+00 09 56	18.60	0.22	1.12	0.0000	3	4863 6562
03.0907	03 02 33.76	+00 10 07	22.20	1.43	1.71	0.5790	1	3933 3969 4102
03.0926	03 02 33.08	+00 08 29	21.91	0.53	2.08	0.3661	4	3727 4959 5007
03.0930	03 02 33.10	+00 09 30	22.22	1.80	2.50	0.2790	1	6562
03.0952	03 02 32.06	+00 08 32	22.49	0.99	13.23	0.8581	3	2799 3727 3933 3969
03.0954	03 02 32.02	+00 08 42	21.77	0.19	4.59	0.0000	3	6562
03.0958	03 02 46.85	+00 07 33	21.75	1.36	1.46	0.0000	2	4304 5175
03.0961	03 02 46.27	+00 07 29	19.92	1.59	4.42	0.0000	2	6159
03.0968	03 02 45.76	+00 05 45	21.74	0.51	2.28	0.3310	4	3727 3934 3969 4863 4959 5007
03.0969	03 02 45.72	+00 06 22	20.75	2.57	2.36	0.8560	3	3933 3969 4000 1
03.0980	03 02 44.86	+00 06 17	22.43	2.11	1.12	0.0000	3	
03.0982	03 02 44.79	+00 06 32	21.26	0.68	2.32	0.1952	4	3727 3969 4863 4959 5007 6562 6725
03.0983	03 02 44.64	+00 06 07	21.01	0.99	3.17	0.3700	3	3934 3969 4102 4304
03.0984	03 02 44.75	+00 07 17	19.29	0.93	2.28	0.7020	3	4000 3969 4304 1
03.0996	03 02 43.22	+00 07 59	22.09	0.63	2.04	0.2193	4	3727 4863 5007 6562 6583 6725
03.0999	03 02 42.69	+00 06 57	21.22	1.58	4.22	0.7040	3	3727 3837 3885 3969 4102 5007

TABLE 1—*Continued*

CFRS	RA[2000]	δ[2000]	I_{AB}[a]	$(V-I)_{AB}$[b]	Q[c]	z	C[d]	Spectroscopic features[e]
03.1014	03 02 41.45	+00 06 17	18.42	0.79	8.91	0.1970	3	4102 4304 5175 6562 6725
03.1016	03 02 40.99	+00 06 55	22.35	0.78	2.71	0.7054	3	3727 3933 3969 1
03.1021	03 02 40.08	+00 05 32	22.24	2.05	3.23	···	0	
03.1027	03 02 39.41	+00 08 13	22.32	1.79	2.39	1.0380	9	3727 1
03.1028	03 02 39.04	+00 06 26	21.22	1.44	1.58	0.0000	3	5175 6562
03.1031	03 02 38.73	+00 05 59	20.68	1.80	1.78	0.4220	3	3885 4304 4863 5175
03.1032	03 02 38.71	+00 06 11	20.49	1.94	1.65	0.6180	4	3727 3969 4102 4304 4863 4959 5007
03.1034	03 02 38.56	+00 07 02	22.20	2.60	1.95	···	0	
03.1035	03 02 38.65	+00 08 15	21.41	1.64	1.86	0.6350	3	3969 4000
03.1046	03 02 36.92	+00 05 57	18.32	0.45	1.44	0.0000	3	4863 5175
03.1050	03 02 36.53	+00 06 16	21.34	0.71	3.96	0.2640	4	3727 3969 4102 4863 4959 5007 6562
03.1051	03 02 36.60	+00 06 53	20.77	0.59	3.58	0.1554	4	3933 3969 4102 4863 4959 5007 6562
03.1056	03 02 36.12	+00 06 51	22.33	1.07	1.76	0.9442	3	2799 3727 4000 4102 1
03.1060	03 02 35.38	+00 06 05	20.88	1.71	1.83	0.4800	3	4000 4102 4304 5175 1
03.1064	03 02 34.59	+00 06 09	21.67	1.39	2.62	0.5750	3	4000 4304 5007
03.1077	03 02 32.59	+00 06 00	20.67	2.13	7.34	0.9380	3	3934 3969 4000 4102
03.1091	03 02 57.70	+00 13 47	21.19	0.98	1.12	···	0	
03.1097	03 02 57.13	+00 12 28	22.40	0.98	2.50	0.1980	3	3969 4863 4959 5007 6562 6725
03.1104	03 02 56.55	+00 13 03	22.22	0.31	1.22	0.1512	4	4863 4959 5007 6562
03.1109	03 02 56.36	+00 14 03	20.21	1.10	1.23	0.2175	4	3933 3969 4000 4304 4863 5175 5892
03.1110	03 02 56.20	+00 12 51	21.52	1.50	2.14	0.3020	1	3969 4304 5175
03.1112	03 02 55.95	+00 12 19	22.03	1.65	3.03	0.7671	3	3727 3969
03.1114	03 02 55.90	+00 14 11	18.67	1.09	1.25	0.2070	3	3933 4000 4304
03.1124	03 02 54.88	+00 12 34	21.51	0.12	3.39	0.1750	3	3969 4102 6562 6725
03.1127	03 02 54.78	+00 12 54	21.60	2.61	1.81	0.0000	4	
03.1128	03 02 54.73	+00 12 53	21.53	2.40	1.05	···	0	
03.1134	03 02 54.29	+00 12 31	21.44	0.47	1.58	0.0000	2	6562
03.1138	03 02 54.01	+00 14 07	22.33	1.19	1.55	0.7663	3	3727 3868
03.1140	03 02 53.85	+00 13 04	21.85	1.12	2.39	1.1818	9	3727
03.1150	03 02 52.94	+00 13 56	20.62	1.84	0.92	0.0000	4	
03.1166	03 02 51.17	+00 14 05	18.81	1.66	1.05	0.0000	4	
03.1168	03 02 50.90	+00 13 53	22.12	0.96	1.59	0.4790	4	3727 4863 4959 5007
03.1171	03 02 50.13	+00 12 26	20.92	2.25	1.46	0.6940	3	3933 3969 4000 4102
03.1175	03 02 49.81	+00 12 41	21.91	1.81	1.12	0.5610	3	3934 3969 4000
03.1179	03 02 49.65	+00 14 16	21.45	0.52	1.79	0.1837	4	3933 3969 4304 4863 4959 5007 6562
03.1184	03 02 49.28	+00 13 37	20.90	0.53	2.79	0.2037	4	3934 3969 4863 5007 6562
03.1206	03 02 58.92	+00 11 36	20.99	1.37	2.26	0.5586	3	3727 3969 4000 4102
03.1213	03 02 58.36	+00 10 36	20.74	2.31	2.22	0.7040	3	3933 3969 4000 4304
03.1217	03 02 57.90	+00 08 33	21.22	0.14	1.98	0.0000	1	4863 6562
03.1220	03 02 57.91	+00 10 43	21.35	2.04	1.95	0.7030	3	3933 3969 4000 4102 4340 1
03.1224	03 02 57.57	+00 09 32	21.48	1.85	1.90	···	0	
03.1228	03 02 57.52	+00 10 27	20.12	2.04	2.45	0.7060	3	3933 3969 4000 4304
03.1242	03 02 56.61	+00 10 49	21.69	1.03	2.62	0.7687	3	3727 3885 3969 4102 4304
03.1243	03 02 56.42	+00 10 43	22.27	1.54	1.73	···	0	
03.1252	03 02 55.66	+00 08 49	22.33	1.58	2.14	···	0	
03.1253	03 02 55.81	+00 10 37	21.69	1.24	2.43	0.5300	4	3727 3933 3969 4102 4863 5175
03.1264	03 02 54.94	+00 08 22	22.34	0.33	1.00	0.0000	1	5175 6562
03.1269	03 02 54.00	+00 08 15	21.55	0.58	2.54	0.3623	3	3727 4959 5007
03.1284	03 02 53.54	+00 10 20	22.13	0.76	1.93	0.9382	3	3727 3933 3969 4000 1
03.1301	03 02 52.42	+00 10 22	22.23	1.84	1.62	0.8410	1	
03.1303	03 02 52.28	+00 09 33	21.61	0.18	1.21	0.0000	3	4863 5175 6562
03.1309	03 02 52.01	+00 10 33	20.62	1.08	4.22	0.6170	4	3727 3837 3934 3969 4304 4863 5175
03.1318	03 02 50.92	+00 10 03	22.29	0.87	1.86	0.8575	9	3727
03.1319	03 02 50.73	+00 08 18	21.51	1.75	2.24	0.6200	4	3727 3934 3969 4102 4304
03.1324	03 02 50.72	+00 10 41	21.80	0.37	4.42	0.1726	3	3969 4304 5007 6562 6725
03.1325	03 02 50.82	+00 11 57	21.58	1.24	2.04	0.5300	1	3727 1
03.1336	03 02 50.03	+00 09 37	19.43	0.61	4.46	0.1759	4	3969 4102 4304 4340 6562 6725
03.1338	03 02 49.98	+00 11 07	20.93	0.71	2.32	0.3763	4	3727 3933 4102 4863 4959 5007 5175
03.1343	03 02 49.56	+00 11 58	21.69	0.40	2.36	0.1887	4	3727 4304 4863 5007 6562
03.1345	03 02 49.22	+00 10 02	21.43	1.65	1.78	0.6167	3	3727 3933 3969 4000 4102
03.1347	03 02 49.00	+00 08 28	20.40	1.63	1.36	0.5620	3	3934 3969 4102 4304 5175
03.1349	03 02 49.08	+00 00 01	20.87	1.29	1.76	0.6155	4	3727 3868 3889 3933
03.1353	03 02 48.39	+00 09 16	21.35	1.53	2.45	0.6340	2	3727 3969
03.1367	03 02 58.64	+00 08 01	22.08	0.50	2.45	0.7053	3	3727 3869 3969 5007
03.1373	03 02 56.98	+00 07 14	20.87	1.71	2.76	0.4825	3	3933 4000 4304 4863 5175 1
03.1375	03 02 56.92	+00 07 06	22.15	0.92	3.00	0.6372	3	3727 3934 3969 4000 4304
03.1381	03 02 55.90	+00 07 07	20.21	1.69	2.52	0.6360	4	3933 3969 4000 4304 4340 1
03.1384	03 02 55.41	+00 06 58	21.52	2.43	4.26	0.7850	2	3933 3969 4000 4304 4340 1
03.1386	03 02 54.71	+00 06 05	20.82	0.18	1.67	···	0	
03.1387	03 02 54.71	+00 06 15	20.62	1.09	1.73	0.2220	1	4304 5175 1
03.1392	03 02 53.45	+00 07 08	20.96	1.49	2.90	0.6050	4	3727 3885 3933 3969 4000 4102 4304
03.1393	03 02 53.12	+00 06 38	22.08	0.86	3.17	0.8520	8	3727
03.1395	03 02 52.94	+00 07 04	22.12	1.42	2.45	0.7080	2	3969 4000 4102
03.1396	03 02 52.57	+00 05 41	22.50	0.78	6.10	0.5565	3	3727 3969 4863 5007
03.1409	03 02 50.47	+00 05 49	21.26	1.92	2.18	0.6182	4	3727 3969 4000 4304 5007 1
03.1413	03 02 49.87	+00 07 15	21.03	1.50	2.32	0.4870	2	4000 4304
03.1416	03 02 49.56	+00 06 14	20.12	1.73	3.35	0.4880	4	3933 3969 4000 4304 4863 1
03.1426	03 02 48.03	+00 06 18	22.21	2.66	3.15	···	0	
03.1428	03 02 47.41	+00 05 58	21.43	1.56	3.23	0.8270	2	3837 3887 3969 4000 4102
03.1441	03 02 29.55	+00 13 23	22.35	1.98	1.79	0.1202	1	5007 5175 6562
03.1480	03 02 23.11	+00 09 52	22.30	2.58	2.59	0.4800	1	3969 4102 4304

TABLE 1—*Continued*

CFRS	RA[2000]	δ[2000]	I_{AB}[a]	$(V-I)_{AB}$[b]	Q[c]	z	C[d]	Spectroscopic features[e]
03.1487	03 02 28.42	+00 07 13	22.22	2.31	1.46	0.2210	1	4863 5892 6562
03.1531	03 02 39.72	+00 13 21	21.81	1.95	3.75	0.7148	3	3727 1
03.1534	03 02 46.84	+00 12 09	22.45	0.70	3.82	0.7977	8	3727
03.1537	03 02 43.37	+00 10 32	21.73	0.83	2.26	···	0	
03.1540	03 02 43.65	+00 12 10	21.04	1.41	2.06	0.6898	3	3727 3969 4863
03.1552	03 02 34.07	+00 10 36	22.47	···	1.37	0.0000	2	
03.1578	03 02 41.96	+00 05 45	21.97	2.05	2.39	···	0	
03.1650	03 02 49.47	+00 08 01	22.00	1.82	2.52	0.6372	3	3727 4000
03.9003	03 02 32.13	+00 06 39	20.77	1.35	3.20	0.6189	4	3727 3837 3885 3933 3969 4102 5007
03.0001	03 02 31.96	+00 14 07	23.00	1.23	13.73	0.8480	92	3969 4000 4102
03.0192	03 02 26.11	+00 09 20	17.47	1.84	0.88	0.0000	94	
03.0220	03 02 24.94	+00 10 07	17.42	0.92	0.90	0.0000	94	5175 5892 6562
03.0358	03 02 26.10	+00 06 23	17.00	1.01	1.10	0.0880	93	5175 6562 6725
03.0368	03 02 25.37	+00 07 32	17.43	1.63	0.88	0.0000	94	
03.0476	03 02 43.11	+00 14 13	21.06	0.40	2.36	0.2597	93	3727 4863 4959 5007
03.0643	03 02 45.73	+00 09 57	23.07	1.05	2.52	0.2710	92	3727 3969 6562
03.0739	03 02 40.81	+00 10 03	22.41	1.01	1.95	0.4800	92	3727 5007
03.0752	03 02 40.18	+00 10 00	17.04	0.14	0.85	0.0000	93	4863 5175 6562
03.0841	03 02 36.82	+00 09 23	16.30	1.22	1.02	0.0000	94	
03.0949	03 02 32.59	+00 12 04	17.48	0.84	5.83	0.0330	94	5007 6562 6725
03.0964	03 02 45.98	+00 05 44	21.26	0.51	2.90	0.3340	94	3727 4863 5007
03.1015	03 02 41.37	+00 05 35	22.90	0.81	2.34	0.6104	93	3727 4863 5007
03.1061	03 02 35.25	+00 06 57	16.80	1.17	0.84	0.0000	94	5175 5892
03.1268	03 02 54.66	+00 09 15	21.58	1.31	1.28	1.0380	99	3727
03.1348	03 02 49.23	+00 10 50	20.58	0.33	1.11	0.0000	93	6562
03.1354	03 02 48.25	+00 09 04	22.05	0.55	2.34	0.8360	93	3727 4340
03.1398	03 02 52.28	+00 07 43	16.83	0.66	0.99	0.0000	94	4863 5175 6562
03.1429	03 02 47.26	+00 07 15	16.49	0.31	0.94	0.0000	94	6562
03.1499	03 02 29.39	+00 06 49	21.54	2.59	2.62	0.8270	93	3933 3969 4000 4102
03.1625	03 02 54.90	+00 10 20	16.15	0.65	0.92	0.0000	94	5175 5892
03.9001	03 02 34.73	+00 09 59	17.41	1.33	8.35	0.0897	94	3933 3969 4304 5892 6562 6527
03.9002	03 02 24.99	+00 06 43	17.05	···	10.61	0.0000	94	

NOTE.—In any use of these data, attention should be paid to the confidence class that has been assigned to each spectroscopic identification. Identifications with $C \leq 1$ are not used in the CFSR scientific analyses described elsewhere. See CFRS II and CFRS III for more information.

[a] Measured in isophotal aperture; see CRFS I.

[b] Measured in a 3″ aperture; see CFRS I.

[c] Compactness parameter; see CFRS I.

[d] Confidence class of the spectroscopic identifications; see CFRS I.

[e] Features noted in the spectra. These are largely self-explanatory, except that a 1 indicates that the continuum shape supported the identification in cases in which the number of distinct features was small and a 2 indicates the multiple features of an M star.

REFERENCES

Crampton, D., Le Fèvre, O., Lilly, S., & Hammer, F. 1995, ApJ, 455, 96 (CFRS V)

Ferguson, H., & McGaugh, S. 1995, ApJ, 440, 470

Le Fèvre, O., Crampton, D., Lilly, S., Hammer, F., & Tresse, L. 1995, ApJ, 455, 60 (CFRS II)

Lilly, S., Hammer, F., Le Fèvre, O., & Crampton, D. 1995, ApJ, 455, 75 (CFRS III)

Lilly, S., Le Fèvre, O., Crampton, D., Hammer, F., & Tresse, L. 1995, ApJ, 455, 50 (CFRS I)

Loveday, J., Peterson, B. A., Efstathiou, G., & Maddox, S. J. 1992, ApJ, 390, 338